Tree Physiology 00, 1–14
doi:10.1093/treephys/tpaa091

Research paper

Amplifying feedback loop between growth and wood anatomical characteristics of *Fraxinus excelsior* explains size-related susceptibility to ash dieback

Stefan Klesse[1,4], Georg von Arx[2], Martin M. Gossner[1,3], Christian Hug[2], Andreas Rigling[2] and Valentin Queloz[1]

[1]Forest Health and Biotic Interactions Department Swiss Federal Research Institute for Forest, Snow, and Landscape Research WSL, Zürcherstrasse 111, 8903 Birmensdorf, Switzerland; [2]Forest Dynamics Department, Swiss Federal Research Institute for Forest, Snow, and Landscape Research WSL, Zürcherstrasse 111, 8903 Birmensdorf, Switzerland; [3]ETH Zurich, Department of Environmental Systems Science, Institute of Terrestrial Ecosystems, Universitätstrasse 8-22, 8092 Zurich, Switzerland; [4]Corresponding author (Stefan.klesse@wsl.ch)

Received February 11, 2020; accepted July 6, 2020; handling Editor Maurizio Mencuccini

Since the 1990s the invasive fungus *Hymenoscyphus fraxineus* has caused severe crown dieback and high mortality rates in *Fraxinus excelsior* in Europe. In addition to a strong genetic control of tolerance to the fungus, previous studies have found landscape heterogeneity to be an additional driver of variability in the severity of dieback symptoms. However, apart from climatic conditions related to heat and humidity influencing fungal infection success, the mechanistic understanding of why smaller or slower-growing trees are more susceptible to dieback remains less well understood. Here, we analyzed three stands in Switzerland with a unique setting of 8 years of data availability of intra-annual diameter growth and annual crown health assessments. We complemented this by ring width and quantitative wood anatomical measurements extending back before the monitoring started to investigate if wood anatomical adjustments can help better explain the size-related dieback phenomenon. We found that slower-growing trees or trees with smaller crowns already before the arrival of the fungus were more susceptible to dieback and mortality. Defoliation directly reduced growth as well as maximum earlywood vessel size, and the positive relationship between vessel size and growth rate caused a positive feedback amplifying and accelerating crown dieback. Measured non-structural carbohydrate (NSC) concentrations in the outermost five rings did not significantly vary between healthy and weakened trees, which translate into large differences in absolute available amount of NSCs. Thus, we hypothesize that a lack of NSCs (mainly sugars) leads to lower turgor pressure and smaller earlywood vessels in the following year. This might impede efficient water transport and photosynthesis, and be responsible for stronger symptoms of dieback and higher mortality rates in smaller and slower-growing trees.

Keywords: basal area increment, Common ash, crown dieback, *Hymenoscyphus fraxineus*, quantitative wood anatomy, tree ring, vessel size.

Introduction

Invasive species increasingly challenge forest and tree health around the world, causing vast socio-economic and ecological impacts (Holmes et al. 2009, Moser et al. 2009, Pyšek and Richardson 2010) as well as reducing forests' capacity to mitigate anthropogenic greenhouse gas emissions (Pan et al. 2011). Ash dieback is a prominent example. This disease is caused by the ascomycete *Hymenoscyphus fraxineus* Baral et al. and threatens populations of Common ash (*F. raxinus excelsior*) throughout Europe. The fungus is native to Eastern Asia (northeastern China, Korea and Japan) and first symptoms were observed in Europe in the early 1990s in northeastern

Poland (Cleary et al. 2016, Gil et al. 2017, Kowalski and Łukomska 2005). Since then the disease has spread fast and is present in most parts of the distribution area of ash in Europe today. Airborne ascospores infect leaves in summer, causing necrotic lesions that lead to early leaf wilting (Gross et al. 2014). If leaves are not shed in time, the fungus further spreads to the xylem through the petiole–shoot junction leading to dieback of shoots and twigs (Hanáčková et al. 2017). Recurring annual infections together with continuing growth of the fungus within the xylem leads to gradual crown dieback and ultimately tree mortality. However, crown dieback symptoms and mortality rates are not uniform among trees. A small proportion of ash trees (5–10%) seems to be tolerant to the disease, and despite very obvious symptoms not all ash trees die after several years of infection (Cleary et al. 2017, Husson et al. 2012, Queloz et al. 2017). It has been shown that late flushing and late senescing trees express significantly stronger dieback symptoms compared with early flushing and early leaf shedding trees (Bakys et al. 2013, McKinney et al. 2011, Muñoz et al. 2016, Pliura et al. 2015, Stener 2013). Early leaf maturation leads to thicker leaf epidermis and cuticle during fungal sporulation and impedes fungal penetration of the leaf cuticle, whereas early leaf shedding reduces the chance of shoot infections. However, the exact mechanism of differential tolerance is not yet understood. But together with additional evidence from common garden experiments (Kjær et al. 2017) the findings support the idea of genetic heritability of tolerance to the fungus (Kjær et al. 2012, Muñoz et al. 2016).

Additionally, there is high variability in crown dieback severity on the landscape level that has been attributed to a variety of commonly reported features: smaller trees (Bengtsson and Stenström 2017, Børja et al. 2017), trees with smaller crown projection area (Gil et al. 2017) and trees of lower social status and under higher competitive pressure were found to be affected most by ash dieback (Enderle et al. 2018). Stand density and local fragmentation seem to also play a crucial role, with trees in less dense stands showing less dieback symptoms compared with denser stands (Bakys et al. 2013), or isolated ash trees being far less affected than trees in forest environment (Grosdidier et al. 2019, Thomsen 2014). There is also consensus that dieback symptoms are less severe in drier and warmer forest stands compared with more humid and cooler forest stands (Chira et al. 2017, Davydenko and Meshkova 2017, Enderle 2019, Ghelardini et al. 2017, Grosdidier et al. 2018, Heinze et al. 2017). Concomitant with crown dieback are strong decreases in radial stem growth (Enderle et al. 2018, Tulik et al. 2018). In line with these observations of crown dieback severity is a meta-analysis of ash mortality surveys across Europe (Coker et al. 2019), where the authors showed that in natural and mature stands the steepest increase in ash mortality happens around 10 years after the first detection of the fungus, leveling off at ~60% mortality. Mortality was found to be higher in young plantations, with ~80% mortality 13 years after first disease detection. Also, Marçais et al. (2017) found that mortality was much higher in small trees (<25 cm diameter at breast height, DBH) compared with larger trees.

Although several observations indicate differences in susceptibility to the fungus related to tree size, the mechanisms why dieback is stronger and mortality is higher in smaller and weaker trees are not well understood. Higher leaf temperatures and lower humidity of sun-exposed crowns of bigger or isolated trees in drier forest stands are likely contributing factors leading to unfavorable or even lethal conditions for infections and mycelial development (Grosdidier et al. 2018, Hauptman et al. 2013, Kowalski and Bartnik 2010, Marçais et al. 2016). In addition, previous dendrochronological studies have shown a significant decline in earlywood vessel size, leading to a less efficient water transport, in dying and already dead trees compared with healthy trees (Tulik et al. 2010, 2017, 2018). However, due to a lack of accompanying crown health assessments in the years prior to their tree core sampling, the mechanisms behind the vessel size reductions remain unclear.

In this study, we analyzed radial growth increment and wood anatomical characteristics related to water transport (earlywood vessel size and theoretical hydraulic conductivity) at three natural ash-dominated stands of varying ages in Switzerland, where *H. fraxineus* was first observed in 2008 (Engesser et al. 2009). We combined tree-ring information with 8 years of annually resolved tree health assessments and asked the following questions: (i) are there differences in tree size, interannual growth increment and wood anatomical characteristics in the pre- and early infection period between trees that are still healthy, and those that already died, or are now severely weakened? (ii) how does ash dieback influence growth and hydraulic efficiency of trees, as well as their interaction?

Material and methods

Study sites

The three studied stands are located near Zürich, Switzerland (47.3577°N, 8.4850°E) at an elevation of 550, 620 and 680 m above sea level, respectively. Climatic conditions are characterized by a mean annual temperature of 8.8 °C and mean annual precipitation sum of 1130 mm (1981–2010). All stands are dominated by European ash (*F. excelsior*) and Sycamore maple (*Acer pseudoplatanus*) with moderately wet clay–loam soils.

The three investigated stands differ in mean tree age ranging from ~33 years (hereafter 'young'), >47 years ('medium'), to 67 years ('old'). In 2011, 60, 104 and 40 trees were tagged at the respective plots and their stem DBH was measured (Figure 1a). On 20 trees of each plot permanent tree girth bands (D1, UMS) were installed at a height of 1.40 m above bark to track their radial increment every 2 weeks from late

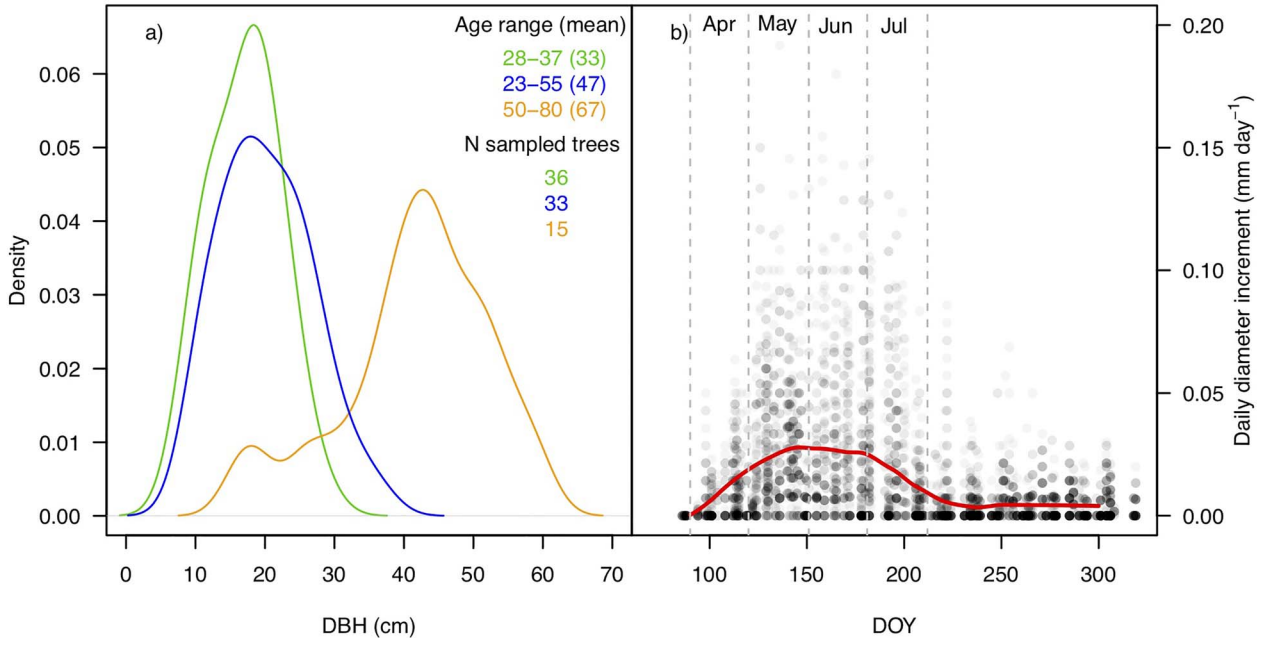

Figure 1. (a) Kernel density distributions of DBH of all tagged trees in 2011 at the three stands. The young stand is colored in green, the medium stand in blue and the old stand in orange. The number of sampled trees and the age range (mean) of the sampled trees are presented in plot-respective colors. (b) Daily diameter increment rates (mm day^{-1}) derived from tree girth bands of 60 trees (20 per plot). The red line shows the modeled mean increment rate (locally estimated regression, span = 0.5), and the gray points represent the individual increment rates. The darker the point, the more data points are superposed.

March to early November from 2012 until 2018. Since 2011 annual crown defoliation (CD) assessments were performed in the middle of August by visually rating the crown transparency in 5% steps ranging from 0% (fully foliated) to 100% (dead; Dobbertin et al. 2004). We classified trees with ≤35% defoliation in 2018 as 'healthy', and those with defoliation between 40 and 95% as 'weak'. Trees that had already died during the monitoring period were classified as 'dead'.

Tree-ring data

In spring 2019 we collected two tree core samples of 5 mm diameter from 84 trees at 1 m height (Figure 1a). At each stand we selected the trees in a stratified random manner covering the full spectrum of healthy, weakened and already dead trees. We leveled the cores with a sledge microtome (WSL core microtome, Gärtner and Nievergelt 2010) and subsequently colored the surface with a black marker and filled vessel lumen with chalk to increase contrast and simplify image analysis. The contrast-enhanced cores were then scanned with a resolution of 2400 dpi (Epson Expression 10000 XL, Seiko Epson Corporation, Japan) and the images analyzed with ROXAS v3.1 (von Arx and Carrer 2014). We excluded vessels smaller 5000 µm^2 from the analysis, because scanning resolution was too low to correctly and automatically identify and measure these small vessels (Figure S1 available as Supplementary Data at *Tree Physiology* Online). Further, it has been shown that these small vessels (that are mainly occurring in the latewood portion of the tree ring) are only responsible for <2% of the total conductivity in another ring-porous species, *Quercus robur* (Fonti et al. 2010). Correct calendar year assignments of tree rings were visually checked, and statistically confirmed with COFECHA (Holmes 1983). Obtained ring widths were transformed to basal area increment (BAI) using the inside-out method, after estimating the distance missing to the pith (R package *dplr*, Bunn et al. 2019). BAI can be primarily interpreted as a latewood width proxy, because in ring-porous species total ring width variability is strongly driven by variation in latewood width (R^2 = 0.93) compared with earlywood width (R^2 = 0.36). For each ring, we pooled the vessel distribution of the two cores and considered vessel hydraulic diameter at the 85th percentile (Dh85, i.e., the widest and thus most conductive vessels, since conductivity increases with vessel diameter at the fourth power) as the parameter related to hydraulic efficiency and the theoretical hydraulic conductivity (Kh; as approximated by Hagen–Poiseuille's law) as a proxy for overall water transport capacity (Tyree and Zimmermann 2002). Dh85 was chosen because early tests revealed the highest signal strength (assessed through highest correlation between trees, Figure S2 available as Supplementary Data at *Tree Physiology* Online) for this percentile of vessel lumen diameter distribution. Because in 41% of all rings the largest vessels were not located in the first row, we decided against analyzing the first row separately, as it is commonly done with most studied ring-porous oak species (González-González et al.

2014, Souto-Herrero et al. 2018). The absolute theoretical hydraulic conductivity (Kh) was obtained by multiplying the ring area-specific theoretical hydraulic conductivity by BAI. Kh is strongly related to total vessel area, which in turn corresponds strongly to earlywood width (Kniesel et al. 2015, Souto-Herrero et al. 2018).

Climate data

Climate data were obtained from the meteorological station in Zürich, downloaded from the KNMI climate explorer (Trouet and Van Oldenborgh 2013). We used monthly mean temperatures and monthly cumulative precipitation covering the 1950–2018 period.

Statistical analysis

BAI, Dh85 and Kh are all dependent on tree size so that our analysis investigating potential differences between tree groups has also to account for this tree size influence (Carrer et al. 2015). Because growth rings within a time series are not independent, we thus modeled BAI, Dh85 and Kh using a linear mixed-effects framework. The effect of tree size on BAI was modeled in Eq. (1):

$$\mathrm{BAI}_{t,j,p} \sim \beta_0 + \beta_1 \mathrm{DBH}_{t-1,j} + \boldsymbol{\beta_{2p}}\boldsymbol{PlotID_p} + \boldsymbol{\beta_{3p}}\mathrm{DBH}_{t-1,j} \times \boldsymbol{PlotID_p} + \gamma_{0,j} + \gamma_{1,j}\mathrm{DBH}_{t-1,j} + \gamma_{2,t,p} + \varepsilon_{t,j,p} \quad (1)$$

where BAI at time t in plot p, tree j, is log-transformed because its variability is proportional to its mean, giving rise to heteroscedasticity in the data. We modeled the effect of log-transformed DBH using a natural cubic spline with a B-spline basis and 2 degrees of freedom, with the knot placed at the median of the variable. The spline adds some more flexibility to the logarithmic function of DBH. It also significantly improved the model fit, as did the interaction of DBH with plotID. DBH is twice the cumulative radius of each sample, summing from the pith. The random year effect γ_2 detects the year-to-year variation common to all samples while determining the influence of DBH on BAI, and essentially serves the same purpose as signal-free detrending in dendrochronology (Melvin and Briffa 2008). Each plot was nested in year to account for differences in stand dynamics of each plot affecting trends in the common interannual signal. Further, we added a random intercept modification (γ_0) and random slope modification (γ_1), capturing variation in the average BAI and size-related trend in BAI among trees caused by unquantified factors such as competition. The scalars β_0, β_1 and the vectors $\boldsymbol{\beta}_{2-3}$, along with the random effects γ_0, γ_1 and γ_2 are regression parameters estimated by the model.

The increase of Dh85 with increasing tree size is mainly attributed to the increasing distance to the apex (Anfodillo et al. 2006). Because we did not measure tree height (and thus distance to the top) and tree height and DBH are highly related, we substituted tree height with DBH. Dh85 and Kh were modeled as follows:

$$\mathrm{DH85}_{t,j,p} \sim \beta_0 + \beta_1 \mathrm{DBH}_{t-1,j} + \boldsymbol{\beta_{2,p}}\boldsymbol{PlotID_p} + \boldsymbol{\beta_{3,p}}\mathrm{DBH}_{t-1,j} \times \boldsymbol{PlotID_p} + \boldsymbol{\gamma_{0,j}} + \boldsymbol{\gamma_{1,j}}DBH_{t-1,j} + \gamma_{2,t,p} + \varepsilon_{t,j,p} \quad (2)$$

$$\mathrm{Kh}_{t,j,p} \sim \beta_0 + \beta_1 \mathrm{DBH}_{t-1,j} + \boldsymbol{\beta_{2p}}\boldsymbol{PlotID_p} + \boldsymbol{\beta_{3p}}\mathrm{DBH}_{t-1,j} \times \boldsymbol{PlotID_p} + \boldsymbol{\gamma_{0,j}} + \boldsymbol{\gamma_{1,j}}DBH_{t-1,j} + \gamma_{2,t,p} + \varepsilon_{t,j,p} \quad (3)$$

In Eqs. (2) and (3) the predictands and DBH are log transformed. We restricted these three analyses to years before 2008 (the official arrival year of the fungus in Switzerland). We then investigated the predisposition of trees to ash dieback by analyzing the differences of DBH, growth (BAI), hydraulic efficiency (Dh85) and theoretical hydraulic conductance (Kh) between the three tree health classes in the 5 years before 2008 using Tukey's post hoc test for multiple comparisons.

To investigate climate drivers of BAI and Dh85, we correlated the random year effects of equations (2) and (3), comprising the common interannual signal of variation while accounting for tree size in BAI and Dh85, respectively, to mean monthly maximum temperatures and monthly precipitation sums over the 1968–2007 period. We conducted the correlation analysis with all possible seasonal window lengths from 1 to 12 months to find the season length with the highest correlation (Klesse et al. 2018). The included months ranged from previous year May to current year September. In a last step, we regressed random year effects of BAI and Dh85 against the two strongest and non-overlapping seasons of both temperature and precipitation and each two-way interaction. We selected the best and simplest model describing interannual variation in BAI, or Dh85, based on the Akaike Information Criterion (Bartoń 2018). We included the most important parameter from these two models in the following analyses to investigate the effect of CD on growth and vessel size during the years 2011–2018.

$$\mathrm{BAI}_{t,j} \sim \beta_0 + \beta_1 T\max_t^{Jun} + \beta_2 \mathrm{DBH}_{t-1,j} + \beta_3 \mathrm{Dh85}_{t,j} + \beta_4 \mathrm{Kh}_{t,j} + \beta_5 \mathrm{CD}_{t,j} + \beta_6 \mathrm{CD}_{t-1,j} + \gamma_j + \varepsilon_{t,j} \quad (4)$$

The effect of CD was modeled using a natural cubic spline with a B-spline basis and 2 degrees of freedom. BAI, DBH, Dh85 and Kh were log transformed (Eq. (4)). PlotID was found to be insignificant to improve model fit and was dropped from the model. Further we modeled Dh85 as:

$$\mathrm{Dh85}_{t,j} \sim \beta_0 + \beta_1 T\max_t^{pJun-Jan} + \beta_2 \mathrm{CD}_{t,j} + \beta_3 \mathrm{CD}_{t-1,j} + \mathrm{BAI}_{t-1,j} + \gamma_j + \varepsilon_{t,j} \quad (5)$$

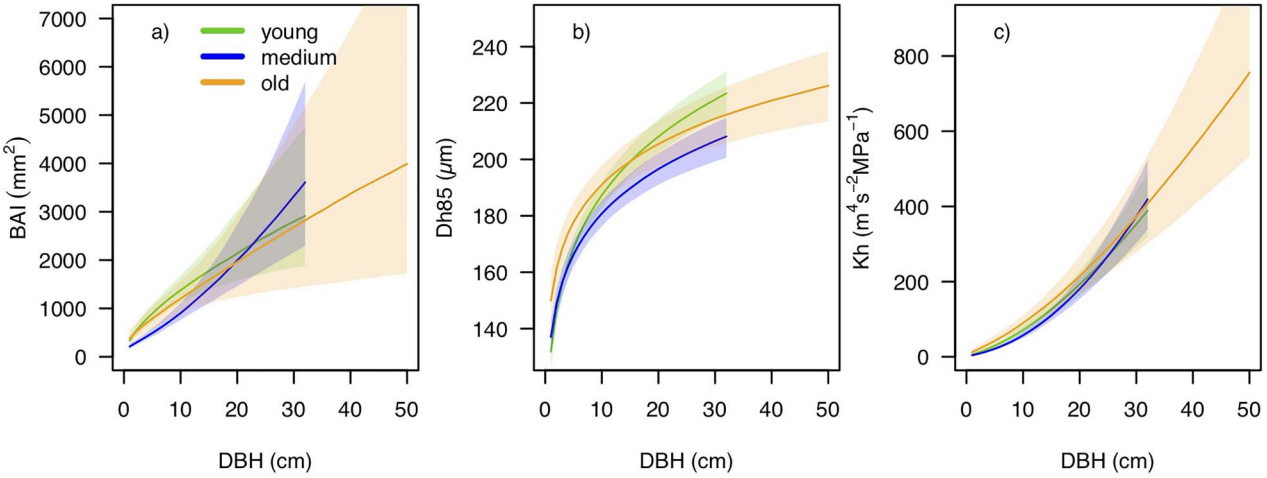

Figure 2. (a) shows the influence of tree DBH on BAI. Shading around solid lines denotes the 95% confidence interval of the fixed effects. Colors represent the three different plots: young (green), medium (blue) and old (orange). (b) Same as (a) but for hydraulic efficiency (Dh85). (c) Same as (a) but for absolute theoretical hydraulic conductivity (Kh).

Dh85 and BAI were log transformed. The inclusion of DBH in Eq. (5) would have led to an erroneous negative effect of DBH on Dh85, a physical impossibility. All models were fit using the *lme4* package (Bates et al. 2015) in R version 3.5.1 R Development Core Team (2016).

Non-structural carbohydrates

We took additional tree cores from 25 trees at 1 m height for the analysis of non-structural carbohydrates (NSCs) before the start of the growing season, at the end of March 2019 between 10.00 and 13.00 h. Samples were dried at 60 °C until a stable weight was achieved and then the outermost 5 years of each core (c.f. von Arx et al. 2017) were ground to a fine powder. NSCs were analyzed following the protocol described by Wong (1990) adapted according to Hoch et al. (2002). This analysis provides an estimate of NSC content per wood dry weight (%NSC) and distinguishes between the contribution of soluble (sugars) and non-soluble carbohydrates (starch). %NSC was calculated for each tree by adding soluble and insoluble carbohydrate contribution.

Results

Of the trees tagged in 2011, 57% had died in the young plot until the end of 2018, whereas in the medium plot only 21% had died. No tagged tree had died until 2018 in the old plot. All three stands had comparable increasing trajectories of tree size-controlled mean growth rate, Dh85 and Kh (Figure 2). The biweekly diameter increment measurements revealed that growth initiation occurred in mid-April and that by the end of July on average 86% of the final diameter increment was completed (Figure 1b).

We found significant differences in DBH, BAI, Dh85 and Kh between the three health classes before the fungus arrived in Switzerland in 2008. Trees that died before 2018 had significantly smaller DBH across all three plots ($P < 0.001$) in 2007, yet, within the plots the difference was not significant. However, these 'dead' trees grew markedly slower, even more so after controlling for tree size compared with healthy trees (all $P < 0.001$, Figure 3a and b). 'Dead' trees also grew slower compared with 'weak' trees, but the differences were not statistically significant. In all three stands and health classes, BAI notably declined after 2008, with strongest declines in weakened trees and trees that subsequently died.

After controlling for tree size Dh85 was significantly higher in 'healthy' trees compared with 'weak' trees ($P < 0.001$), yet not significantly higher compared with 'dead' trees ($P = 0.07$, Figure 4a and b). Also, Dh85 declined in all health classes since 2008, yet we observed weakest decreases in the 'healthy' class.

Kh was significantly different between the healthy and dead trees (Figure 5a). After controlling for tree size, differences were still significant between the weak/dead and healthy trees (Figure 5b). Similar to BAI and Dh85, Kh declined in all health classes after 2008.

Interannual variation in the 1968–2007 period of BAI was negatively impacted by mean maximum temperatures in June, the period of maximum growth rates (c.f. Figure 1b; $r = -0.39$). Dh85 was strongly and positively influenced by mean maximum temperatures of previous year June to current year January (partial correlation coefficient: 0.51) and current year April–June temperatures ($r = 0.48$), and cumulative precipitation of previous year December to current year March ($r = 0.38$; total adjusted explained variance: 0.57, Figure S3a available as Supplementary Data at *Tree Physiology* Online). The relationships were also present after high-pass filtering all four time series

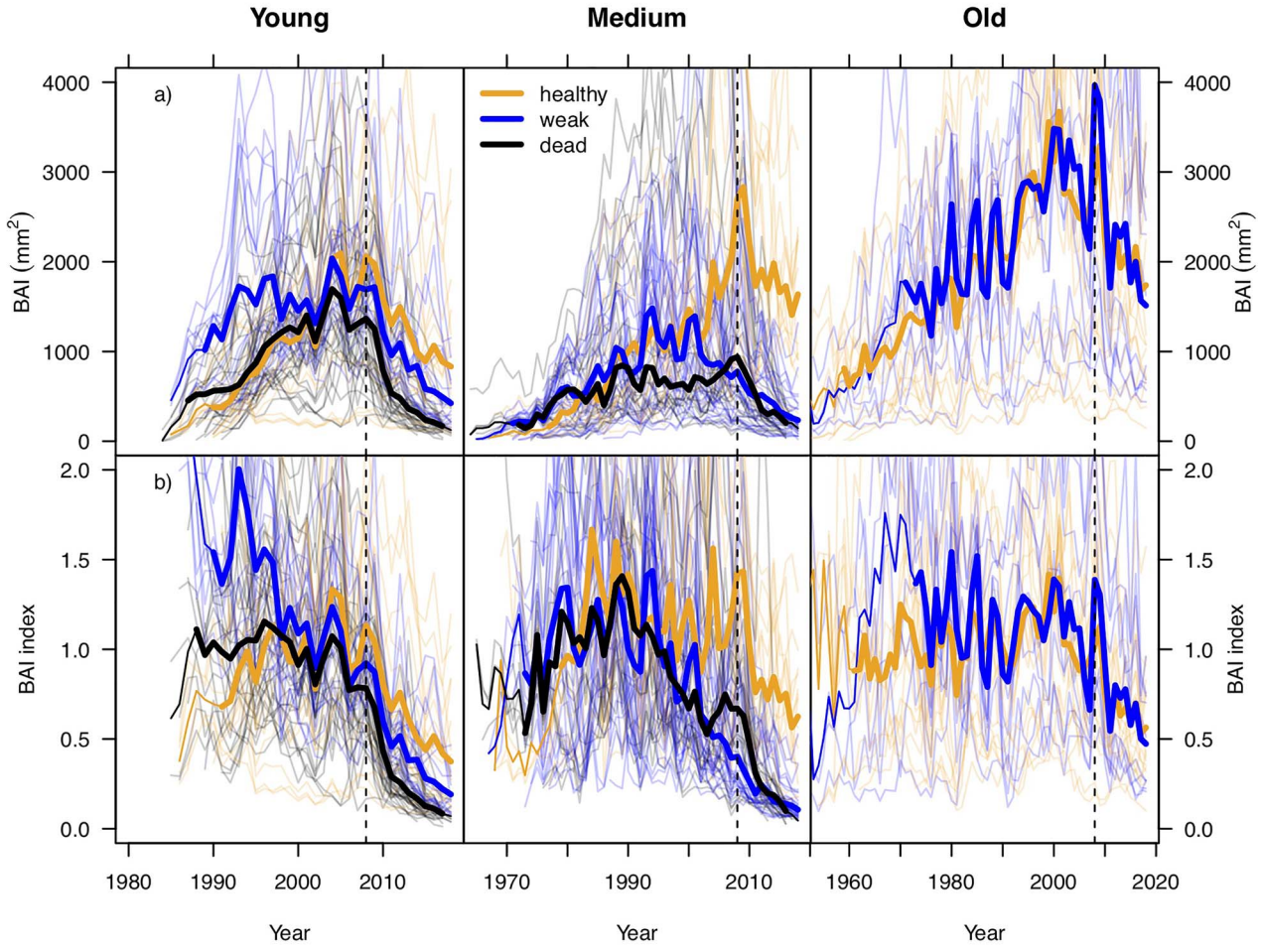

Figure 3. (a) Raw BAI time series and (b) BAI time series controlled for the effect of DBH on BAI (model 1), modeled without random effects. Orange lines show time series of trees that had 35% or less defoliation in 2018, blue lines denote weakened trees (>35–95% defoliation) and black lines represent BAI of trees that had died until 2018. The bold lines are group-specific mean time series (averaged with Tukey's biweight robust mean), they are thinned in the early years, when sample replication drops <10. The vertical dashed line at 2008 marks the first observation of the fungus in Switzerland.

using a cubic smoothing spline with a 50% frequency cutoff at 10 years, yet slightly lower (0.46, 0.45, 0.31; adjR^2 = 0.37), showing the robustness of these relationships (Figure S3b available as Supplementary Data at *Tree Physiology* Online).

Defoliation of previous year and current year had a very strong negative impact on BAI, whereas Dh85 had a significant positive effect (Figure 6a). Together with Kh and previous fall and winter mean maximum temperatures, these fixed effects variables explained 79% (marginal R^2) of the variance in BAI (conditional R^2 including random effects explained 93% of the variance). The model predicts a 66% reduction of productivity at 50% defoliation. Defoliation also had a negative impact on Dh85, whereas BAI of previous year positively affected Dh85 (Figure 6b, R^2m:0.47, R^2c:0.73). Per 10% reduction in foliage Dh85 decreases by ~5 µm. Thus, given a Dh85 of 200 µm, a 50% defoliation causes a 12.5% decrease in Dh85, leading to a loss of conductivity of Dh85 by 41% (Hagen–Poseuille's law). Since defoliation also causes BAI to decrease, and a decreased BAI in the previous year simultaneously negatively affects Dh85 (dashed lines in Figure 6b), the realistic ring-level reduction of conductivity at 50% defoliation is closer to 55%. We did not find significant differences in NSC concentration of the outermost five rings between healthy and weakened trees (P = 0.1, Figure 7), although there was a tendency toward lower values in weakened trees. Also, differences in starch and sugar concentrations were insignificant (P = 0.07 and 0.89, respectively).

Discussion

In this study, we showed for the first time the direct negative impact of annually resolved fungal-caused defoliation on radial growth and earlywood vessel size. Our analyses further confirm previous observations that small and weak trees are more prone

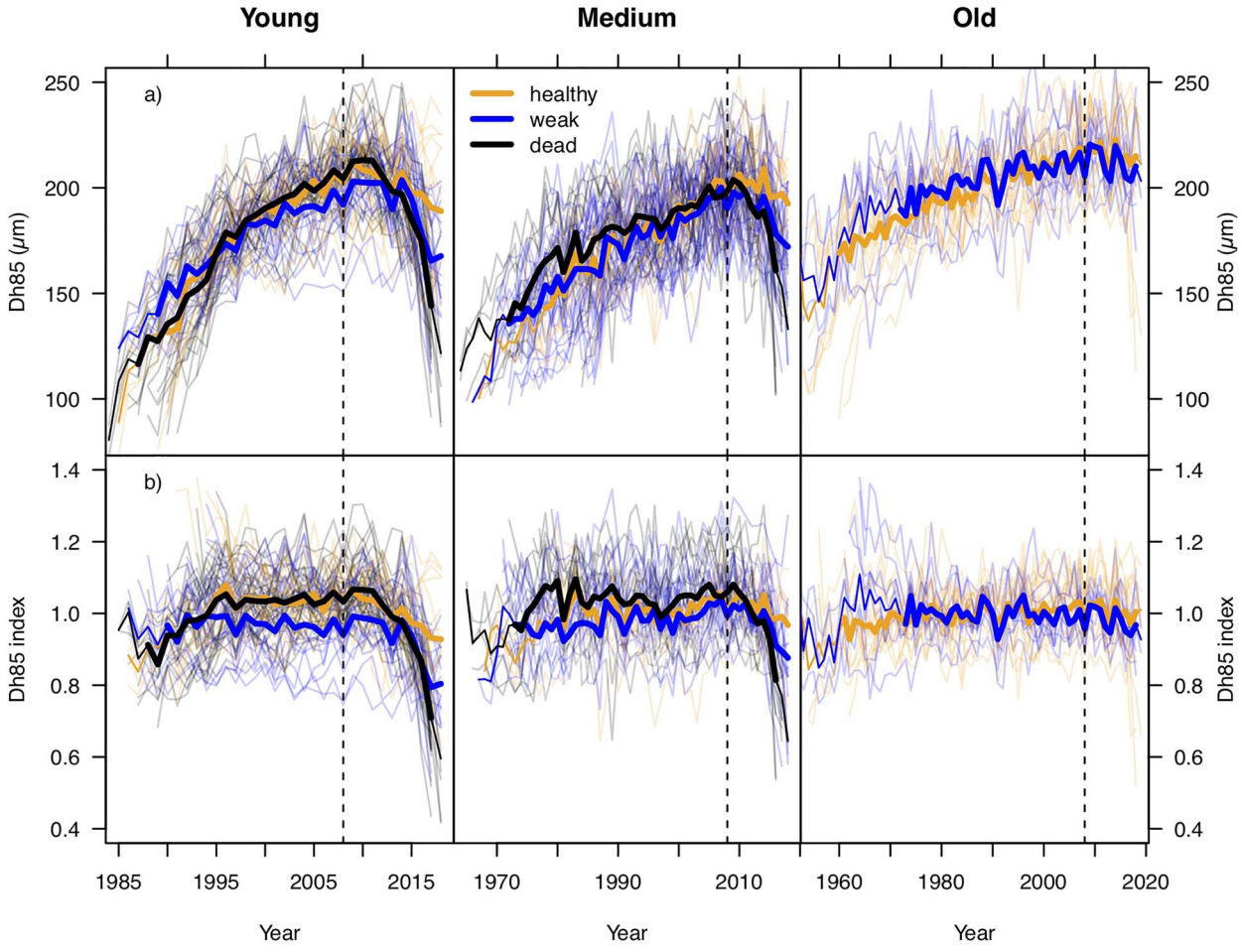

Figure 4. (a) Raw hydraulic efficiency (Dh85) time series and (b) Dh85 time series controlled for DBH modeled without random effects (model 2). Lines and colors as in Figure 1.

to dieback and associated mortality and also allowed us to draw inferences about the mechanisms. In the following, we discuss how the reduction in crown size, associated growth reduction and reduction in maximum vessel size (affecting hydraulic efficiency) interact and may hint at missing stored carbohydrates as a probable cause for accelerated dieback in small and/or slow-growing trees.

Predisposition to crown dieback

Trees that are dead or weakened today had lower BAI compared with relatively healthy-looking trees (Figure 3a) in the years before the fungus arrived. This pattern was true not only in absolute growth terms (raw BAI) but also when controlling for tree size (Figure 3b). This confirms previous studies (Enderle 2019), showing small and weak trees (with lower social status and higher competition) are succumbing first to the fungal attack and that tall trees with big crowns show less fungus-induced crown dieback. Stronger dieback in trees with low growth rates due to higher competition would be in line with the observation that shading effects favor fungal infection and development compared with fully sun-exposed crowns (Grosdidier et al. 2018, Kowalski and Bartnik 2010).

Defoliation and associated decrease in growth and vessel size

In our studied trees, radial growth is almost finished at the end of July (Figure 1b), a finding supported by other automatic dendrometer measurements of *F. excelsior* (Brinkmann et al. 2016, Köcher et al. 2012, Mund et al. 2010) and xylogenesis data of another central European ring-porous species, *Quercus petraea* (Michelot et al. 2012). Leaf shedding occurs in the middle of October, which leaves two and a half months to produce carbohydrates primarily allocated to storage (Chapin et al. 1990, Kozlowski 1992). Fungal-induced necrotic lesions on leaves usually develop during these last months of the growing season. It has been shown in other plants that necrotic lesions on leaves strongly impede photosynthesis (Erickson et al. 2004, Gruber et al. 2012, Roloff et al. 2004). As the

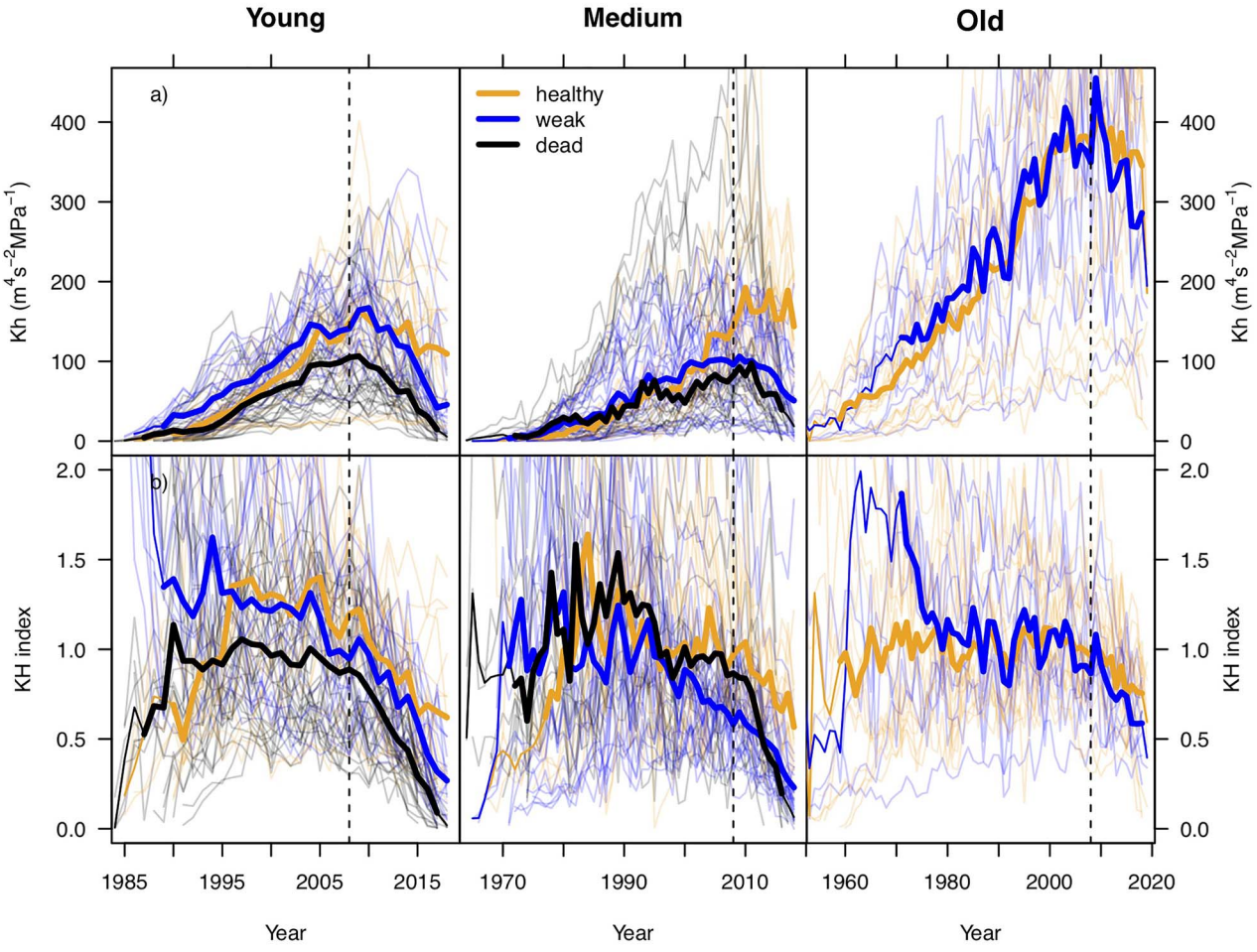

Figure 5. (a) Raw absolute theoretical hydraulic conductivity (Kh) time series and (b) Kh time series controlled for DBH modeled without random effects (model 3). Lines and colors as in Figure 1.

fungus can also grow within the twigs and kill shoots and buds, it potentially leads to a smaller crown in the next year. Defoliation thus reduces photosynthetic capacity by reducing the total leaf area, inevitably reducing radial growth. Reduced photosynthesis decreases also the ability to produce and store NSC, primarily as starch, toward the end of the growing season (Furze et al. 2019, Martínez-Vilalta et al. 2016). Indeed, it has been shown that artificial defoliation in July strongly decreased starch concentration in shoots and roots in saplings of *Acer saccharum* (Gregory and Wargo 1986).

Increasing vessel size with increasing distance to the apex is a well-known feature (Zasada and Zahner 1969) and is proposed to being the most efficient anatomical adjustment for stabilizing hydraulic path-length resistance (Anfodillo et al. 2013). As a consequence of the ash dieback disease, twigs and branches from the periphery die back and tree heights are progressively reduced. As such, it could thus be expected that the observed reduction in Dh85 is a result of a decrease in hydraulic path length. However, the observed decrease in Dh85 from ~210 to ~150 µm (Figures 4a and 6b) is too strong to be purely attributable to a reduction in path length. Based on three dead trees that we sampled along the stem, a Dh85 of 150 µm is achieved at distances to the apex of 3–5 m (equivalent to a 4.3–6.3 m tall tree; Figure S4 available as Supplementary Data at *Tree Physiology* Online) or when the trees are <5 cm in DBH. The crown base (the first bifurcation of the main branches forming the crown) of those trees is with 8–10 m at least 4 m higher, where we could at least expect Dh85 of >170 µm. Due to the strong log–log relationship between Dh and path length, Dh increases only slightly at path lengths (or tree heights) >10 m (Anfodillo et al. 2006, 2013), whereas the majority of axial conduit widening occurs in the first 10 m of tree height growth (i.e., the first 10 m from the top). For this reason, we find it unlikely to primarily attribute the decrease in Dh85 to a decrease in tree height.

The potential role of NSCs in dieback severity

Cell enlargement in trees is largely a turgor-driven process, which depends on water potential and osmotic potential (Cabon et al. 2020, Woodruff et al. 2004, Woodruff and Meinzer 2011).

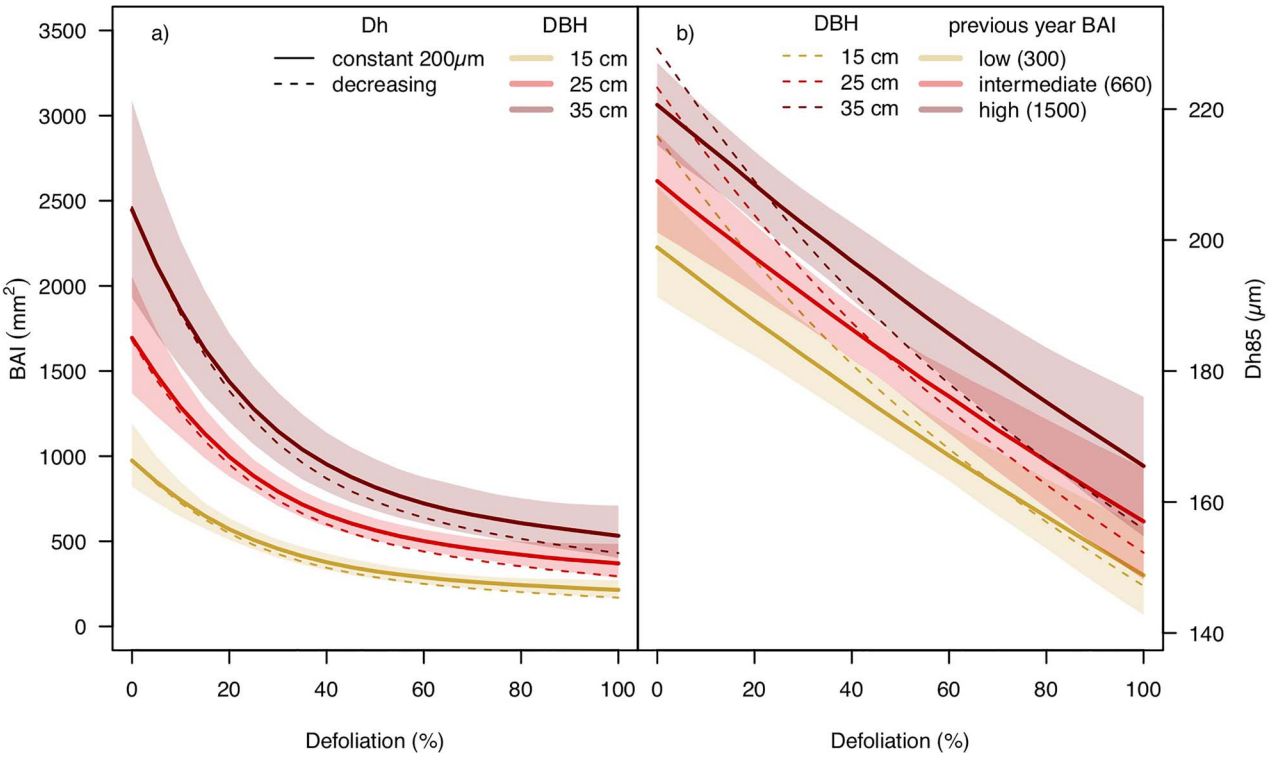

Figure 6. (a) Modeled effect of mean defoliation of current and previous year on BAI. Different colors are modeled effects at different DBH. Solid lines show the effect with a constant Dh85 of 200 µm. Shading around solid lines denotes the 95% confidence interval of the fixed effects. The dashed lines show the initiated feedback on BAI when vessel size (Dh85) decreases simultaneously 5 µm per 10% defoliation. This decrease in Dh85 with increasing defoliation was extracted from the model shown in (b). (b) Effect of mean defoliation of current and previous year on Dh85. Solid lines show modeled effects at constant previous year's BAI, representing the median, the 25th and the 75th percentile of BAI during the 2011–2018 period. Shading around solid lines denotes the 95% confidence interval of the fixed effects. The dashed lines show the effect of defoliation with concomitant decrease in previous year's BAI at given DBH, initiating a positive feedback loop with Dh85. Theoretical BAI values at given DBH with increasing defoliation were extracted from the model shown in (a). The yellow (red; brown) line represents a tree with 15 cm (25; 35 cm) DBH.

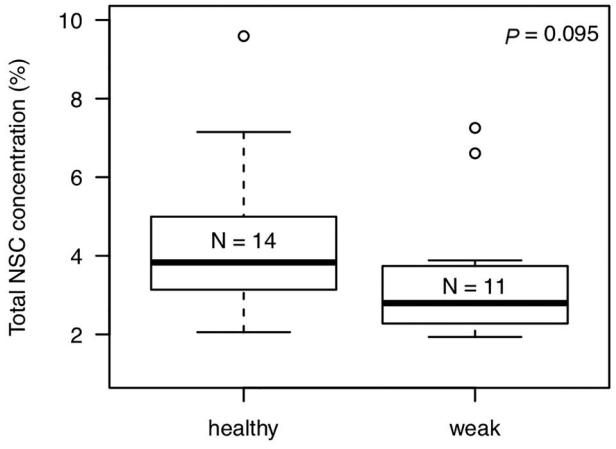

Figure 7. Distribution of NSC content per wood dry weight (%NSC) of 14 healthy and 11 weakened trees, and *P* value of Wilcoxon rank-sum test. Thick horizontal line denotes the median, boxes show the interquartile range (IQR), whiskers extend to 1.5 times the IQR. Circles are outliers.

Earlywood vessel formation in the ring-porous European ash begins several weeks before leaf flushing (Atkinson and Denne 1988, Frankenstein et al. 2005, Sass-Klaassen et al. 2011). These vessels are thus entirely produced by carbon reserves. Reduced turgor pressure due to a lack of stored carbohydrates or a lack of water could thus lead to smaller vessels, less efficient water transport hampering photosynthesis and respiration and ultimately reduce the capacity to produce wood, new shoots and to put up defense mechanisms against the fungus. This is particularly true for ring-porous species, since only the earlywood vessels in the outermost ring are functional and account for almost the entire water transport (Cochard and Tyree 1990, Davis et al. 1999, Utsumi et al. 1999), i.e., the trees are not able to compensate smaller earlywood vessels by higher numbers in older, previously formed rings. It has been shown that trees with smaller vessel sizes—i.e., with less efficient water transport—and trees with lower theoretical hydraulic conductivity (Kh) have lower photosynthetic rates (Choat et al. 2011, Hubbard et al. 2001, Katul et al. 2003, Rust and Roloff 2002, Santiago et al. 2004, Zhang and Cao 2009). This explains our finding that both higher Kh, which is also a potential sign for a larger crown, and higher Dh85 positively influence BAI (Figure 6). A similar observation was made also by Fan et al. (2012) and Hoeber

et al. (2014) who found a strong positive relationship between Dh and Kh and radial growth rates in the tropics.

The observed positive correlation of Dh85 to mean maximum temperatures of previous fall and winter, and spring, and the positive correlation to winter precipitation adds to the hypothesis that a lack of turgor pressure leads to smaller vessels. High temperatures from June to October enable high photosynthetic rates and thus a high potential to produce and store carbohydrates after secondary growth has finished. Warmer winter temperatures might lower NSC consumption due to less conversion of starch to sugar-based frost protection compounds (Sperling et al. 2015). At the onset of the growing season trees would have more carbohydrates available to create osmotic potential to enlarge vessels.

Warm early growing season temperatures (April–June) are indicative for higher meristem activity and higher enzymatic activity to extract stored carbohydrates (Parent et al. 2010). A positive relationship between vessel size and early spring temperatures (during the onset of vessel formation) was also previously shown in chestnut in Ticino, Switzerland (Fonti et al. 2007). Therefore, April temperatures were related to tree activation through new hormone production leading to changes in the auxin gradient that facilitates the expansion of vessels (Aloni 2010, Uggla et al. 1996). Positive correlations between maximum vessel size with mean monthly temperatures in May were also found in two oak species in southwestern Quebec, Canada (Tardif and Conciatori 2006) and in oaks in northwestern Spain (Souto-Herrero et al. 2017, 2018).

Water-saturated soils positively influence stem water potential for formation of new vessels (Deleuze and Houllier 1998, Fritts et al. 1991). The observed positive influence of winter precipitation on vessel size can thus be attributed to wetter soils in spring favoring the enlargement of vessels. A similar observation was made by Castagneri et al. (2017) in two mediterranean oak species in Israel. The observed climate–vessel size relationships all point toward a slight increase in vessel size over time. We can thus rule out climate-induced changes being responsible for the observed decreases in vessel size, also under the aspect that defoliation affects vessel size more strongly than mean maximum temperature of previous June to current year January (i.e., the combined effect of defoliation of current and previous year is more than seven times as high, Table S1 available as Supplementary Data at *Tree Physiology* Online, equation (5)).

We did not find that trees producing smaller earlywood vessels are more prone to decline as described by Tulik et al. (2010). However, we found a tendency that relative Kh (Kh controlled for tree size) and absolute Kh of the dying and already dead trees were lower already before 2008 compared with healthy trees (Figure 5). Low Kh is indicative for a smaller crown and thus lower productivity. Trees with smaller crowns likely produce smaller rings, and thus less wood to store carbohydrates for the next year. Lower Kh through a combination of less vessels and smaller vessels leads to a progression in crown dieback (Pellizzari et al. 2016). This is another argument for the potentially crucial role of NSCs (sugars) in dieback severity.

Large trees typically have a higher increment (BAI or volume increment) than smaller trees and thus a higher volume to store carbohydrates in the outermost rings. It has further been shown that NSC concentration decreases strongly with increasing distance from cambium (Hoch et al. 2003). The effect was found to be particularly strong in ring-porous *Q. petraea*. Also, von Arx et al. (2017) found an initial decrease in NSC concentration (mainly driven by changes in sugar concentration) in irrigated *Pinus sylvestris* and their non-irrigated, drought-stressed and slower-growing control group with increasing distance from the cambium. They found no difference in NSC concentration between the two groups but due to twice as high growth rates of the irrigated trees their total NSC pool of the outermost 5 years was twice as big. Schönbeck et al. (2018) analyzed a similar set of trees on the same study site and found that with increasing defoliation sugar concentration decreased. Because their study analyzed a fixed amount of wood (2 cm) compared with von Arx et al. (2017), who analyzed a fixed number of rings (groups of 5 years), the observed decrease in NSC concentration with increasing defoliation had to be influenced by the higher number of rings in slower-growing and stronger defoliated trees. These findings are in contrast to Pacheco et al. (2018) that analyzed the outermost 5 cm of *Pinus halepensis* in Spain and found lower NSC concentrations in fast-growing irrigated trees, indicating possible ecosystem- and species-specific responses.

In our case, we did not find significant differences in NSC concentration between healthy and weakened trees (Figure 7) in the outermost 5 years. Hence, lower growth rate would be directly proportional to a lower amount of stored carbohydrates that can be remobilized out of a certain volume of wood. This lower amount of mobilized sugars consequently would negatively influence the maximum earlywood vessel size and thus reduce hydraulic efficiency and conductivity, hamper photosynthesis and finally accelerate fungal-induced crown dieback and mortality.

Concluding, we showed that fungal-induced defoliation not only reduces growth, but also directly decreases maximum earlywood vessel size. Smaller vessels reduce the efficiency of water transport, which negatively affects photosynthesis and radial growth. Low radial growth in turn also affects vessel sizes in the following year, which leads to a positive, amplifying feedback that accelerates crown dieback. Our finding that slower-growing trees or trees with smaller crowns already before the arrival of the fungus seem to be more susceptible to crown dieback further supports this idea. It also indicates that sylvicultural measures like thinning could be a useful management tool to mitigate impacts on ash by *H. fraxineus*. Reducing stand density

would reduce shading, consequently fungal performance and enhance growth of the promoted trees.

Our results further lead us to the hypothesis that a lack of NSCs (sugars) is responsible for smaller and slower-growing trees showing stronger symptoms of fungal-induced dieback and higher mortality rates. Future analyses of stable isotope ratios of oxygen, carbon and hydrogen could give further insight into the mechanisms of photosynthesis, stomatal conductance and carbon reserve remobilization during fungal-induced crown dieback and thus contribute to a more holistic understanding of the ways of European ash to fight, cope with or succumb to the fungus.

Supplementary Data

Supplementary Data for this article are available at *Tree Physiology* online.

Data and materials availability

Data and materials will be made available upon reasonable request.

Acknowledgments

The authors thank Richard Peters for discussion, and the numerous colleagues involved in fieldwork monitoring girth increment and assessing crown health.

Conflict of interest

None declared.

Funding

SwissForestLab project #3 to S.K.

Authors' Contributions

S.K. designed the study with the input of M.G., A.R. and V.Q. S.K. performed the analyses and wrote the first draft of the manuscript. All authors commented critically on all versions of the manuscript.

References

Aloni R (2010) The induction of vascular tissues by auxin. In: Davies PJ (ed) Plant hormones: biosynthesis, signal transduction, action! Springer, Dordrecht, pp 485–518.

Anfodillo T, Carraro V, Carrer M, Fior C, Rossi S (2006) Convergent tapering of xylem conduits in different woody species. New Phytol 169:279–290.

Anfodillo T, Petit G, Crivellaro A (2013) Axial conduit widening in woody species: a still neglected anatomical pattern. IAWA J 34:352–364.

von Arx G, Arzac A, Fonti P, Frank D, Zweifel R, Rigling A, Galiano L, Gessler A, Olano JM (2017) Responses of sapwood ray parenchyma and non-structural carbohydrates of *Pinus sylvestris* to drought and long-term irrigation. Funct Ecol 31:1371–1382.

von Arx G, Carrer M (2014) ROXAS – a new tool to build centuries-long tracheid-lumen chronologies in conifers. Dendrochronologia 32:290–293.

Atkinson CJ, Denne MP (1988) Reactivation of vessel production in ash (*Fraxinus excelsior* L.) trees. Ann Bot 61:679–688.

Bakys R, Vasaitis R, Skovsgaard JP (2013) Patterns and severity of crown dieback in young even-aged stands of European ash (*Fraxinus excelsior* L.) in relation to stand density, bud flushing phenotype, and season. Plant Prot Sci 49:120–126.

Bartoń K (2018) MuMIn: multi-model inference. R package version 1.42.1. https://CRAN.R-project.org/package=MuMIn (2 February 2020, date last accessed).

Bates D, Mächler M, Bolker B, Walker S (2015) Fitting linear mixed-effects models using lme4. J Stat Softw 67:1–48.

Bengtsson V, Stenström A (2017) Ash dieback - a continuing threat to veteran ash trees?) In: Vasaitis R, Enderle R (eds) Dieback of European ash (*Fraxinus* spp) - consequences and guidelines for sustainable management, Swedish University of Agricultural Sciences, Uppsala, Sweden, pp 262–272.

Børja I, Timmermann V, Hietala AM, Tollefsrud MM, Nagy NE, Vivian-Smith A, Cross H, Myking T, Solheim H (2017) Ash dieback in Norway – current situation. In: Vasaitis R, Enderle R (eds) Dieback of European ash (*Fraxinus* spp) - consequences and guidelines for sustainable management, Swedish University of Agricultural Sciences, Uppsala, Sweden, pp 166–175.

Brinkmann N, Eugster W, Zweifel R, Buchmann N, Kahmen A (2016) Temperate tree species show identical response in tree water deficit but different sensitivities in sap flow to summer soil drying. Tree Physiol 36:1508–1519.

Bunn A, Korpela M, Biondi F, Campelo F, Mérian P, Qeadan F, Zang C (2019) dplR: Dendrochronology Program Library in R. R package version 1.7.0. https://CRAN.R-project.org/package=dplR (2 February 2020, date last accessed).

Cabon A, Fernández-de-Uña L, Gea-Izquierdo G, Meinzer FC, Woodruff DR, Martínez-Vilalta J, Cáceres MD (2020) Water potential control of turgor-driven tracheid enlargement in scots pine at its xeric distribution edge. New Phytol 225:209–221.

Carrer M, von Arx G, Castagneri D, Petit G (2015) Distilling allometric and environmental information from time series of conduit size: the standardization issue and its relationship to tree hydraulic architecture. Tree Physiol 35:27–33.

Castagneri D, Regev L, Boaretto E, Carrer M (2017) Xylem anatomical traits reveal different strategies of two Mediterranean oaks to cope with drought and warming. Environ Exp Bot 133:128–138.

Chapin FS, Schulze E-D, Mooney HA (1990) The ecology and economics of storage in plants. Annu Rev Ecol Syst 21:423–447.

Chira D, Chira F, Tăut I et al. (2017) Evolution of ash dieback in Romania. In: Vasaitis R, Enderle R (eds) Dieback of European Ash (Fraxinus spp) - consequences and guidelines for sustainable management, Swedish University of Agricultural Sciences, Uppsala, Sweden, pp 185–194.

Choat B, Medek DE, Stuart SA, Pasquet-Kok J, Egerton JJG, Salari H, Sack L, Ball MC (2011) Xylem traits mediate a trade-off between resistance to freeze–thaw-induced embolism and photosynthetic capacity in overwintering evergreens. New Phytol 191:996–1005.

Cleary M, Nguyen D, Marčiulynienė D, Berlin A, Vasaitis R, Stenlid J (2016) Friend or foe? Biological and ecological traits of the European ash dieback pathogen *Hymenoscyphus fraxineus* in its native environment. Sci Rep 6:1–11.

Cleary M, Nguyen D, Stener LG, Stenlid J, Skovsgaard JP (2017) Ash and ash dieback in Sweden: a review of disease history, current status, pathogen and host dynamics, host tolerance and management options

in forests and landscapes. In: Vasaitis R, Enderle R (eds) Dieback of European Ash (Fraxinus spp) - consequences and guidelines for sustainable management, Swedish University of Agricultural Sciences, Uppsala, Sweden, pp 195–208.
Cochard H, Tyree MT (1990) Xylem dysfunction in Quercus: vessel sizes, tyloses, cavitation and seasonal changes in embolism. Tree Physiol 6:393–407.
Coker TLR, Rozsypálek J, Edwards A, Harwood TP, Butfoy L, Buggs RJA (2019) Estimating mortality rates of European ash (*Fraxinus excelsior*) under the ash dieback (*Hymenoscyphus fraxineus*) epidemic. Plants People Planet 1:48–58.
Davis SD, Sperry JS, Hacke UG (1999) The relationship between xylem conduit diameter and cavitation caused by freezing. Am J Bot 86:1367–1372.
Davydenko K, Meshkova V (2017) Dieback of European ash (*Fraxinus* spp) - consequences and guidelines for sustainable management. In: Vasaitis R, Enderle R (eds) The current situation concerning severity and causes of ash dieback in Ukraine caused by *Hymenoscyphus fraxineus*, Swedish University of Agricultural Sciences, Uppsala, Sweden, pp 220–227.
Deleuze C, Houllier F (1998) A simple process-based xylem growth model for describing wood microdensitometric profiles. J Theor Biol 193:99–113.
Dobbertin M, Hug C, Mizoue N (2004) Using slides to test for changes in crown defoliation assessment methods. Part I: visual assessment of slides. Environ Monit Assess 98:295–306.
Enderle R (2019) An overview of ash (*Fraxinus* spp.) and the ash dieback disease in Europe. CAB Rev 14:1–12.
Enderle R, Metzler B, Riemer U, Kändler G (2018) Ash dieback on sample points of the National Forest Inventory in South-Western Germany. Forests 9:25.
Engesser R, Queloz V, Meier F, Kowalski T, Holdenrieder O (2009) Das Triebsterben der Esche in der Schweiz. Wald und Holz 90:24–27.
Erickson JE, Stanosz GR, Kruger EL (2004) Photosynthetic consequences of Marssonina leaf spot differ between two poplar hybrids. New Phytol 161:577–583.
Fan Z-X, Zhang S-B, Hao G-Y, Slik JWF, Cao K-F (2012) Hydraulic conductivity traits predict growth rates and adult stature of 40 Asian tropical tree species better than wood density. J Ecol 100:732–741.
Fonti P, Solomonoff N, García-González I (2007) Earlywood vessels of *Castanea sativa* record temperature before their formation. New Phytol 173:562–570.
Fonti P, von Arx G, García-González I, Eilmann B, Sass-Klaassen U, Gärtner H, Eckstein D (2010) Studying global change through investigation of the plastic responses of xylem anatomy in tree rings. New Phytol 185:42–53.
Frankenstein C, Eckstein D, Schmitt U (2005) The onset of cambium activity – a matter of agreement? Dendrochronologia 23:57–62.
Fritts HC, Vaganov EA, Sviderskaya IV, Shashkin AV (1991) Climatic variation and tree-ring structure in conifers: empirical and mechanistic models of tree-ring width, number of cells, cell size, cell-wall thickness and wood density. Clim Res 1:97–116.
Furze ME, Huggett BA, Aubrecht DM, Stolz CD, Carbone MS, Richardson AD (2019) Whole-tree nonstructural carbohydrate storage and seasonal dynamics in five temperate species. New Phytol 221:1466–1477.
Gärtner H, Nievergelt D (2010) The core-microtome: a new tool for surface preparation on cores and time series analysis of varying cell parameters. Dendrochronologia 28:85–92.
Ghelardini L, Migliorini D, Santini A et al. (2017) From the Alps to the Apennines: possible spread of ash dieback in Mediterranean areas. In: Vasaitis R, Enderle R (eds) Dieback of European ash (*Fraxinus* spp) - consequences and guidelines for sustainable management, Swedish University of Agricultural Sciences, Uppsala, Sweden, pp 140–149.
Gil W, Kowalski T, Kraj W, Zachara T, Łukaszewicz J, Paluch R, Nowakowska JA, Oszako T (2017) Ash dieback in Poland - history of the phenomenon and possibilities of its limitation. In: Vasaitis R, Enderle R (eds) Dieback of European Ash (Fraxinus spp) - consequences and guidelines for sustainable management, Swedish University of Agricultural Sciences, Uppsala, Sweden, pp 176–184.
González-González BD, Rozas V, García-González I (2014) Earlywood vessels of the sub-Mediterranean oak *Quercus pyrenaica* have greater plasticity and sensitivity than those of the temperate *Q. petraea* at the Atlantic–Mediterranean boundary. Trees 28:237–252.
Gregory RA, Wargo PM (1986) Timing of defoliation and its effect on bud development, starch reserves, and sap sugar concentration in sugar maple. Can J For Res 16:10–17.
Grosdidier M, loos R, Marçais B (2018) Do higher summer temperatures restrict the dissemination of *Hymenoscyphus fraxineus* in France? For Pathol 48:e12426.
Grosdidier M, Scordia T, Loos R, Marçais B (2019) Landscape epidemiology of ash dieback. bioRxiv 582080.
Gross A, Holdenrieder O, Pautasso M, Queloz V, Sieber TN (2014) *Hymenoscyphus pseudoalbidus*, the causal agent of European ash dieback. Mol Plant Pathol 15:5–21.
Gruber BR, Kruger EL, McManus PS (2012) Effects of cherry leaf spot on photosynthesis in tart cherry 'Montmorency' foliage. Phytopathology 102:656–661.
Hanáčková Z, Havrdová L, Černy K, Zahradník D, Koukol O (2017) Fungal endophytes in ash shoots – diversity and inhibition of *Hymenoscyphus fraxineus*. Balt For 23:19.
Hauptman T, Piškur B, de GM, Ogris N, Ferlan M, Jurc D (2013) Temperature effect on *Chalara fraxinea*: heat treatment of saplings as a possible disease control method. For Pathol 43:360–370.
Heinze B, Tiefenbacher H, Litschauer R, Kirisits T (2017) Ash dieback in Austria - history, current situation and outlook. In: Vasaitis R, Enderle R (eds) Dieback of European ash (*Fraxinus* spp) - consequences and guidelines for sustainable management, Swedish University of Agricultural Sciences, Uppsala, Sweden, pp 33–52.
Hoch G, Popp M, Körner C (2002) Altitudinal increase of mobile carbon pools in *Pinus cembra* suggests sink limitation of growth at the Swiss treeline. Oikos 98:361–374.
Hoch G, Richter A, Körner C (2003) Non-structural carbon compounds in temperate forest trees. Plant Cell Environ 26:1067–1081.
Hoeber S, Leuschner C, Köhler L, Arias-Aguilar D, Schuldt B (2014) The importance of hydraulic conductivity and wood density to growth performance in eight tree species from a tropical semi-dry climate. For Ecol Manage 330:126–136.
Holmes RL (1983) Computer-assisted quality control in tree-ring dating and measurement. Tree-Ring Bull 43:69–78.
Holmes TP, Aukema JE, Holle BV, Liebhold A, Sills E (2009) Economic impacts of invasive species in forest past, present, and future. Annals of the New York Academy of Sciences 1162:18–38.
Hubbard RM, Ryan MG, Stiller V, Sperry JS (2001) Stomatal conductance and photosynthesis vary linearly with plant hydraulic conductance in ponderosa pine. Plant Cell Environ 24:113–121.
Husson C, Caël O, Grandjean JP, Nageleisen LM, Marçais B (2012) Occurrence of *Hymenoscyphus pseudoalbidus* on infected ash logs. Plant Pathol 61:889–895.
Katul G, Leuning R, Oren R (2003) Relationship between plant hydraulic and biochemical properties derived from a steady-state coupled water and carbon transport model. Plant Cell Environ 26:339–350.
Kjær ED, McKinney LV, Hansen LN, Olrik DC, Lobo A, Thomsen IM, Hansen JK, Nielsen LR (2017) Genetics of ash dieback resistance in a restoration context - experiences from Denmark. In: Vasaitis R, Enderle R (eds) Dieback of European ash (*Fraxinus* spp) - consequences and guidelines for sustainable management, Swedish University of Agricultural Sciences, Uppsala, Sweden, pp 106–114.

Kjær ED, McKinney LV, Nielsen LR, Hansen LN, Hansen JK (2012) Adaptive potential of ash (*Fraxinus excelsior*) populations against the novel emerging pathogen *Hymenoscyphus pseudoalbidus*. Evol Appl 5:219–228.

Klesse S, Babst F, Lienert S et al. (2018) A combined tree ring and vegetation model assessment of European forest growth sensitivity to interannual climate variability. Global Biogeochem Cycles 32:1226–1240.

Kniesel BM, Günther B, Roloff A, von Arx G (2015) Defining ecologically relevant vessel parameters in *Quercus robur* L. for use in dendroecology: a pointer year and recovery time case study in Central Germany. Trees 29:1041–1051.

Köcher P, Horna V, Leuschner C (2012) Environmental control of daily stem growth patterns in five temperate broad-leaved tree species. Tree Physiol 32:1021–1032.

Kowalski T, Bartnik C (2010) Morphological variation in colonies of *Chalara fraxinea* isolated from ash (*Fraxinus excelsior* L.) stems with symptoms of dieback and effects of temperature on colony growth and structure. Acta Agrobot 63:99–106.

Kowalski T, Łukomska A (2005) The studies on ash dying (*Fraxinus excelsior* L.) in the Włoszczowa Forest Unit stands. https://pubag.nal.usda.gov/catalog/5239646 (3 February 2020, date last accessed).

Kozlowski TT (1992) Carbohydrate sources and sinks in woody plants. Bot Rev 58:107–222.

Marçais B, Husson C, Caël O, Dowkiw A, Delahaye L, Collet C, Chanderlier A (2017) Estimation of ash mortality induced by *Hymenoscyphus fraxineus* in France and Belgium. Balt For 23:159–167.

Marçais B, Husson C, Godart L, Caël O (2016) Influence of site and stand factors on *Hymenoscyphus fraxineus*-induced basal lesions. Plant Pathol 65:1452–1461.

Martínez-Vilalta J, Sala A, Asensio D, Galiano L, Hoch G, Palacio S, Piper FI, Lloret F (2016) Dynamics of non-structural carbohydrates in terrestrial plants: a global synthesis. Ecol Monogr 86: 495–516.

McKinney LV, Nielsen LR, Hansen JK, Kjær ED (2011) Presence of natural genetic resistance in *Fraxinus excelsior* (Oleraceae) to *Chalara fraxinea* (Ascomycota): an emerging infectious disease. Heredity 106:788–797.

Melvin TM, Briffa KR (2008) A "signal-free" approach to dendroclimatic standardisation. Dendrochronologia 26:71–86.

Michelot A, Simard S, Rathgeber C, Dufrêne E, Damesin C (2012) Comparing the intra-annual wood formation of three European species (*Fagus sylvatica*, *Quercus petraea* and *Pinus sylvestris*) as related to leaf phenology and non-structural carbohydrate dynamics. Tree Physiol 32:1033–1045.

Moser WK, Barnard EL, Billings RF et al. (2009) Impacts of nonnative invasive species on US forests and recommendations for policy and management. J For 107:320–327.

Mund M, Kutsch WL, Wirth C, Kahl T, Knohl A, Skomarkova MV, Schulze E-D (2010) The influence of climate and fructification on the interannual variability of stem growth and net primary productivity in an old-growth, mixed beech forest. Tree Physiol 30:689–704.

Muñoz F, Marçais B, Dufour J, Dowkiw A (2016) Rising out of the ashes: additive genetic variation for crown and collar resistance to *Hymenoscyphus fraxineus* in *Fraxinus excelsior*. Phytopathology 106:1535–1543.

Pacheco A, Camarero JJ, Carrer M (2018) Shifts of irrigation in Aleppo pine under semi-arid conditions reveal uncoupled growth and carbon storage and legacy effects on wood anatomy. Agric For Meteorol 253–254:225–232.

Pan Y, Birdsey RA, Fang J et al. (2011) A large and persistent carbon sink in the World's forests. Science 333:988–993.

Parent B, Turc O, Gibon Y, Stitt M, Tardieu F (2010) Modelling temperature-compensated physiological rates, based on the co-ordination of responses to temperature of developmental processes. J Exp Bot 61:2057–2069.

Pellizzari E, Camarero JJ, Gazol A, Sangüesa-Barreda G, Carrer M (2016) Wood anatomy and carbon-isotope discrimination support long-term hydraulic deterioration as a major cause of drought-induced dieback. Glob Chang Biol 22:2125–2137.

Pliura A, Lygis V, Marčiulyniene D, Suchockas V, Bakys R (2015) Genetic variation of *Fraxinus excelsior* half-sib families in response to ash dieback disease following simulated spring frost and summer drought treatments. iForest 9:12.

Pyšek P, Richardson DM (2010) Invasive species, environmental change and management, and health. Annu Rev Env Resour 35:25–55.

Queloz V, Hopf S, Schoebel CN, Rigling D, Gross A (2017) Ash dieback in Switzerland: history and scientific achievements. In: Vasaitis R, Enderle R (eds) Dieback of European ash (*Fraxinus* spp) - consequences and guidelines for sustainable management, Swedish University of Agricultural Sciences, Uppsala, Sweden, pp 68–78.

R Development Core Team (2016) R: a language and environment for statistical computing. R Foundation for Statistical Computing, Vienna, Austria.

Roloff I, Scherm H, van Iersel MW (2004) Photosynthesis of blueberry leaves as affected by Septoria leaf spot and abiotic leaf damage. Plant Dis 88:397–401.

Rust S, Roloff A (2002) Reduced photosynthesis in old oak (*Quercus robur*): the impact of crown and hydraulic architecture. Tree Physiol 22:597–601.

Santiago LS, Goldstein G, Meinzer FC, Fisher JB, Machado K, Woodruff D, Jones T (2004) Leaf photosynthetic traits scale with hydraulic conductivity and wood density in Panamanian forest canopy trees. Oecologia 140:543–550.

Sass-Klaassen U, Sabajo CR, den Ouden J (2011) Vessel formation in relation to leaf phenology in pedunculate oak and European ash. Dendrochronologia 29:171–175.

Schönbeck L, Gessler A, Hoch G, McDowell NG, Rigling A, Schaub M, Li M-H (2018) Homeostatic levels of nonstructural carbohydrates after 13 yr of drought and irrigation in *Pinus sylvestris*. New Phytol 219:1314–1324.

Souto-Herrero M, Rozas V, García-González I (2017) A 481-year chronology of oak earlywood vessels as an age-independent climatic proxy in NW Iberia. Global Planet Change 155:20–28.

Souto-Herrero M, Rozas V, García-González I (2018) Earlywood vessels and latewood width explain the role of climate on wood formation of *Quercus pyrenaica* Willd. Across the Atlantic-Mediterranean boundary in NW Iberia. For Ecol Manage 425:126–137.

Sperling O, Earles JM, Secchi F, Godfrey J, Zwieniecki MA (2015) Frost induces respiration and accelerates carbon depletion in trees. PLoS One 10:e0144124.

Stener L-G (2013) Clonal differences in susceptibility to the dieback of *Fraxinus excelsior* in southern Sweden. Scand J For Res 28:205–216.

Tardif JC, Conciatori F (2006) Influence of climate on tree rings and vessel features in red oak and white oak growing near their northern distribution limit, southwestern Quebec, Canada. Can J For Res 36:2317–2330.

Thomsen IM (2014) Das Eschentriebsterben an Stadt- und Straßenbäumen. In: Dujesiefken D (ed) Jahrbuch der Baumpflege 2014., pp 103–109.

Trouet V, Van Oldenborgh GJ (2013) KNMI climate explorer: a web-based research tool for high-resolution paleoclimatology. Tree-Ring Res 69:3–13.

Tulik M, Marciszewska K, Adamczyk J (2010) Diminished vessel diameter as a possible factor in the decline of European ash (*Fraxinus excelsior* L.). Ann For Sci 67:103–103.

Tulik M, Yaman B, Köse N (2018) Comparative tree-ring anatomy of *Fraxinus excelsior* with Chalara dieback. J For Res 29:1741–1749.

Tulik M, Zakrzewski J, Adamczyk J, Tereba A, Yaman B, Nowakowska JA (2017) Anatomical and genetic aspects of ash dieback: a look at the wood structure. iForest 10:522.

Tyree MT, Zimmermann MH (2002) Xylem structure and the ascent of sap. Springer, Berlin, Heidelberg.

Uggla C, Moritz T, Sandberg G, Sundberg B (1996) Auxin as a positional signal in pattern formation in plants. PNAS 93:9282–9286.

Utsumi Y, Sano Y, Funada R, Fujikawa S, Ohtani J (1999) The progression of cavitation in earlywood vessels of *Fraxinus mandshurica* var japonicaduring freezing and thawing. Plant Physiol 121:897–904.

Wong S-C (1990) Elevated atmospheric partial pressure of CO2 and plant growth. Photosynth Res 23:171–180.

Woodruff DR, Bond BJ, Meinzer FC (2004) Does turgor limit growth in tall trees? Plant Cell Environ 27:229–236.

Woodruff DR, Meinzer FC (2011) Size-dependent changes in biophysical control of tree growth: the role of turgor. In: Meinzer FC, Lachenbruch B, Dawson TE (eds) Size- and age-related changes in tree structure and function. Springer, Dordrecht, pp 363–384.

Zasada JC, Zahner R (1969) Vessel element development in the earlywood of red oak (*Quercus rubra*). Can J Bot 47:1965–1971.

Zhang J-L, Cao K-F (2009) Stem hydraulics mediates leaf water status, carbon gain, nutrient use efficiencies and plant growth rates across dipterocarp species. Funct Ecol 23:658–667.